Journal of Nanotechnology & Advanced Materials
An International Journal

http://dx.doi.org/10.18576/jnam/050204

Influence of HCl Treatement on Porous Silicon for Optoelectronic Applications

I. Rathinamala[1], N. Jeyakumaran[2] and N. Prithivikumaran[2,]*

[1]Department of Physics, V.V.Vanniaperumal College for Women, Virudhunagar – 626001, Tamilnadu, India.
[2]Nanoscience Research Lab, Department of Physics, VHNSN College, Virudhunagar – 626001, Tamilnadu, India.

Received: 9 May 2016, Revised: 25 Dec. 2016, Accepted: 31 Dec. 2016.
Published online: 1 Jul. 2017.

Abstract: In the present work p-type (1 0 0) oriented silicon wafers were used to form porous structures by electrochemical anodization method. Electrochemically etched porous silicon (PS) samples were exposed to an HCl solution for set time intervals, resulting in a stable and enhanced luminescence from this material. SEM, EDAX, XRD, FTIR and PL studies were carried out to understand the role of HCl on the PS substrates. Scanning electron micrographs demonstrate the profound change that accompanies the HCl treatment of the PS surface. The porosity of the PS was determined using the SEM images by geometric method. Effective medium approximation method reveals that the refractive index decreases with porosity. When the samples are anodized with HCl content in the electrolyte; there is a net decrease in the concentration of the Si-H groups on the material surface. Strong visible emission peak at 498 nm, with no apparent shift with respect to variation in etching parameter, is observed in photoluminescence study.

Keywords: PS/HCl, SEM, porosity, Refractive index, FTIR, PL.

1 Introduction

Porous silicon (PS) consists of a network of nanoscale sized silicon wires and voids which formed when crystalline silicon wafers are etched electrochemically in hydrofluoric acid based electrolyte solution under constant anodization conditions. The precise control of porosity and thickness allows the tailoring of optical properties of porous silicon and has opened the door to a multitude of applications in optoelectronics technology.

Porous silicon has attracted great attention due to its room temperature photoluminescence in the visible light range [1]. However, two different hypotheses are reported on photoluminescence from porous silicon surface. The first includes the quantum confinement effect which is due to the charge carriers in narrow crystalline silicon wall separating the pore walls and the second is due to the presence of luminescent surface species trapped in the inner walls as the source light emission and the third one is due to the presence of surface confined molecular emitters i.e. siloxene [2-5]. The role of the surface passivation is very important in determining the radiative efficiency of the porous layer [6]. Porous silicon structures have good mechanical robustness, chemical stability and compatibility with existing silicon technology and therefore have a wide area of potential applications such as waveguides, 1D photonic crystals, chemical sensors, biological sensors, photovoltaic devices etc. [7-13]. Several physical quantities of porous silicon such as refractive index, photoluminescence and electrical conductivity change drastically on exposure of chemical substances.

In this work, synthesis and characterization study of electrochemically anodized nanocrystalline porous silicon layers were done. The influence of post etch treatment of HCl over the properties of porous silicon (PS) is also studied.

2 Experimental Methods

2.1 Fabrication of Porous Silicon

PS samples were prepared by electrochemical etching using silicon as the anode and platinum as the counter electrode in an acid-resistant Teflon single tank system. Boron doped, single crystalline, 0 -100 Ωcm resistivity, p-type (1 0 0) silicon

*Corresponding author e-mail: janavi_p@yahoo.com

© 2017 NSP
Natural Sciences Publishing Cor.

wafer was used for preparing PS. The wafers were cleaned in acetone for 5 minute ultrasonically and then with deionized water. The PS synthesis was done at 50 mA/cm^2 current density under 10 minute etching time in an electrolytic solution of aqueous hydrofluoric acid and ethanol. The role of ethanol during the etching process is to lower the surface tension of the electrolyte. It also minimizes hydrogen bubble formation at silicon/electrolyte interface during anodization and does not disturb the transport of ions towards and away from the interface, thereby, improving layer uniformity. Good homogeneity within the PS layers was obtained because the electrical contact to the silicon substrate is made on the entire back surface of the wafer which prevents lateral potential variation across the wafer that would cause changes in the local current density. In the present work the electrochemical etching of silicon was done at room temperature. The schematic of electrochemical etching setup used in the work is shown in the Fig. 1.

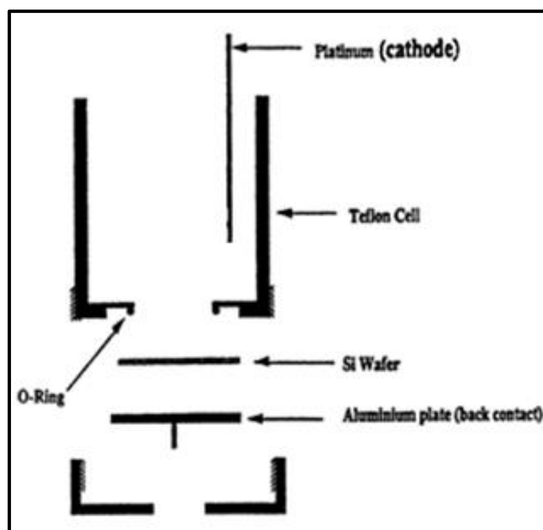

Figure. 1. The schematic of porous silicon etching setup

2.2 Formation of Hydrochloric acid Treated Porous Silicon (PS/HCl)

The surface passivation of porous silicon plays a significant role in emission efficiency of the material. Therefore, the electrochemically etched porous silicon (PS) samples were exposed to 3 M HCl solution for set time duration such as 1, 5, 10, 20, 40 and 60 minute seperately. The method includes treating the PS substrate with an aqueous hydrochloric acid solution and then the etched PS substrate is rinsed with alcohol. The development of porosity produced by the chemical activation yields an increase in the volume of micropores.

PS samples were analyzed in a Hitachi scanning microscope (models 450) operated at 15 kV and photographed. X – Ray diffraction (XRD) patterns were obtained using X'PERT PRO X – ray diffractometer, which was operated at 40 KV and 30 mA with CuKα_1 radiation of wavelength 1.5407 Å. The Fourier Transform Infra Red (FTIR) spectra of the samples have been obtained using the Shimadzu FTIR-8400S spectrometer in the wave number range of 2800 – 400 cm^{-1} with a resolution of 4 cm^{-1}. The photoluminescence (PL) spectra of the samples were recorded using Perkin Elmer LS 55 Luminescence Spectrometer in the emission wavelength range of 400 – 800 nm, fixing the excitation wavelength at 450 nm. All the measurements were carried out at room temperature.

3 Results

3.1 SEM and EDAX Analysis

Fig. 2 shows the scanning electron micrograph images of porous silicon sample with HCl content in the electrolytes for different etching time. Scanning Electron Micrograph of PS shows well - defined pores created due to anodic etching with very distinct boundaries.

Porous silicon samples are composed of sponge-like network channels, which support a myriad of microscopic protuberances in the form of clusters located all over the internal surfaces of the pores. Such pores may be expected to exhibit quantum confinement effects leading to increase in the effective energy gap. Scanning electron micrographs demonstrate the profound change that accompanies the HCl treatment of the PS surface.

Fig. 3 shows the EDAX spectrum of HCl treated Porous Silicon. In the spectrum, the chlorine could possibly from residues of the HCl acid used for pore widening treatment.

© 2017 NSP
Natural Sciences Publishing Cor.

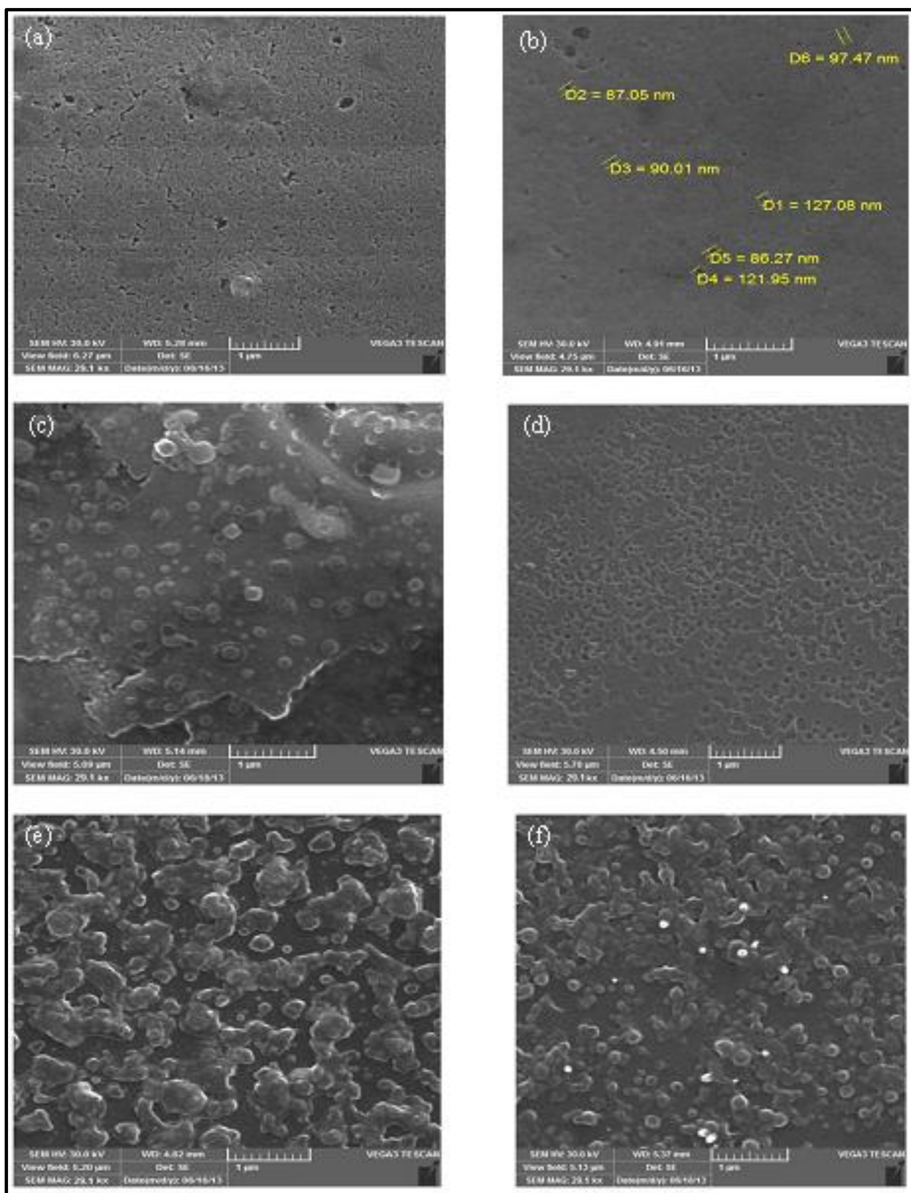

Figure. 2. SEM images of HCl treated Porous Silicon a) 1 minute b) 5 minute c) 10 minute d) 20 minute e) 40 minute f) 60 minute

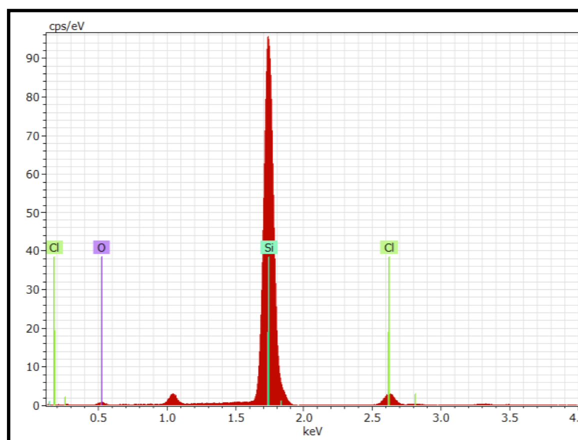

Figure. 3. EDAX spectra of HCl treated Porous Silicon

© 2017 NSP
Natural Sciences Publishing Cor.

The porosity plays a key role in photoluminescence properties of the porous silicon layer. The porosity of the porous silicon is defined as the quantity of silicon removed during anodization compared with the silicon concentration before anodization evaluated in the same volume [14]. The porosity (P) can also be defined as a function of geometrical parameters and it can be written as,

$$P = \left(\frac{\pi}{2} * 1.732\right)\left[\frac{1}{(1+m/d)}\right]^2 \quad (1)$$

where 'd' is the average pore size and m is the distance between the pores. The calculated porosity values from SEM images with respect to etching time are plotted in Fig.4. It was found that the porosity increases by the treatment of HCl.

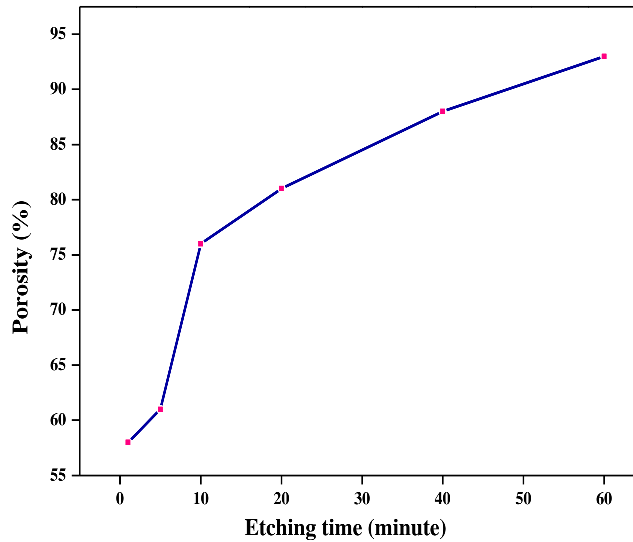

Figure. 4. Variation of porosity with HCl etching time

3.2 Refractive index determination using an effective medium approximation

The porous silicon with uniformly distributed pore is modeled considering it as a two or three phase system. In cases where the typical length scale characterizing feature sizes of the topology is much smaller than the light wavelength one can neglect the retardation effects and apply an effective medium theory to replace the two component system of pore walls and pores by associating an effective medium with a macroscopic so called effective dielectric function ε_{eff} [15]. Theoretical determination of ε_{eff} depends on the dielectric constants of the constituents and the nanostructure of the system consisting of the silicon, voids and passivated surfaces. Various assumptions about the pore morphology may lead to different model predicting dielectric constant as a function of the porosity. The equations given by Maxwell-Garnett [16], Bruggeman [17] and Looyenga [18] methods are used to determine refractive index as a function of porosity and are given below as equations (2), (3) and (4) respectively.

$$(1-\mathrm{P})\frac{n_{Si}{}^2 - n_{air}{}^2}{n_{Si}{}^2 + 2n_{air}{}^2} = \frac{n_{PS}{}^2 - n_{air}{}^2}{n_{PS}{}^2 + 2n_{air}{}^2} \quad (2)$$

$$\mathrm{n}_{PS} = 0.5\left[3P\left(1-\mathrm{n_{Si}}^2\right) + (2\mathrm{n_{Si}}^2 - 1) + \left[(3P\left(1-\mathrm{n_{Si}}^2\right) + (2\mathrm{n_{Si}}^2 - 1))^2 + 8n_{Si}{}^2\right]^{0.5}\right]^{o.5} \quad (3)$$

$$\mathrm{n}_{PS}{}^{2/3} = (1\text{-P})\ \mathrm{n}_{Si}{}^{2/3} + \mathrm{P}\ \mathrm{n_{air}}^{2/3} \quad (4)$$

where P is the porosity, n_{PS}, n_{air} and n_{Si} is the refractive indices of porous silicon, air and silicon respectively. The calculated refractive index values are given in Table 1.

Fig. 5 shows a comparison between refractive index values of Maxwell-Garnett, Bruggeman and Looyenga effective medium approximation methods as a function of porosity. From this graph, it is clear that the refractive indices of porous particles decrease with the growth of porosity.

© 2017 NSP
Natural Sciences Publishing Cor.

Table. 1: Calculated values of refractive index using effective medium approximation methods

Porosity P (%)	Refractive Index n		
	Maxwell-Garnett Method	Bruggeman Method	Looyenga Method
58	1.574	1.845	1.913
61	1.546	1.807	1.841
76	1.329	1.344	1.490
81	1.235	1.299	1.389
88	1.133	1.153	1.220
93	1.084	1.091	1.138

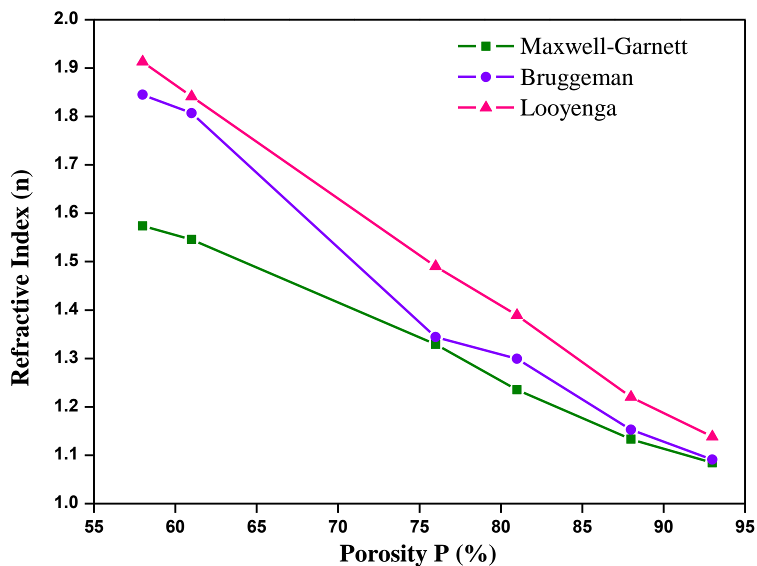

Figure. 5. Refractive index as a function of porosity

3.3 XRD Analysis

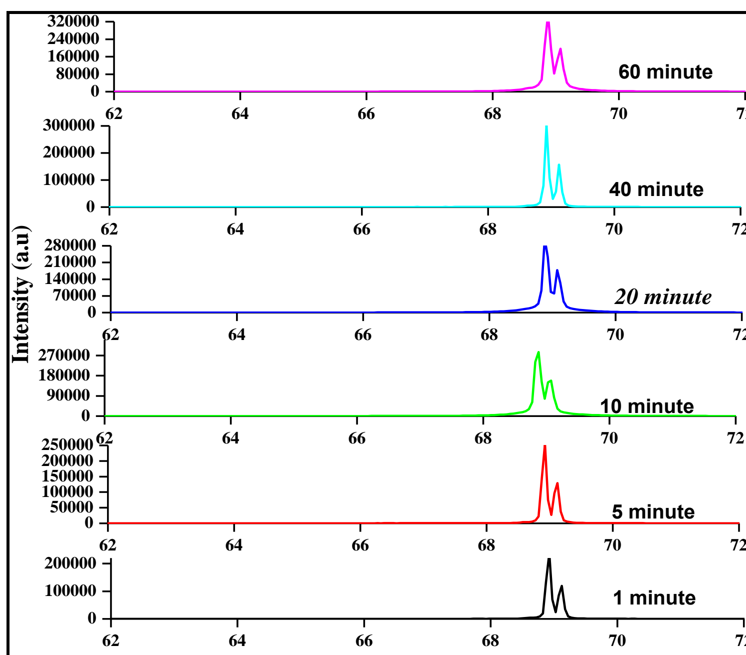

Figure. 6. XRD spectra of HCl treated porous silicon for different etching time

© 2017 NSP
Natural Sciences Publishing Cor.

The XRD pattern of all the PS structures (Fig. 6) exhibited a dominant diffraction peak at 2θ = 68.9° corresponding to the (4 0 0) plane (JCPDS File No. 89 – 2955) and is due to crystalline Si substrates. Another trivial peak at 69.1° is due to the porous layer [19]. The crystallite size was calculated using Debye–Scherrer formula.

The values of crystallite size obtained from XRD pattern were 140 nm, 124 nm, 118 nm, 99 nm, 97 nm and 81 nm for HCl treated PS layer for the different HCl treating times given by 1, 5, 10, 20, 40 and 60 minute respectively. It is also observed that the FWHM value of the PS increases with the etching time of HCl and these values are listed in Table 2.

Table. 2: Calculated values of crystallite size and FWHM of PS with HCl etching treatment

HCl etching time (minute)	Porosity P (%)	Crystallite Size (nm)	FWHM
1	58	140	0.0717
5	61	124	0.0810
10	76	118	0.0851
20	81	99	0.1013
40	88	97	0.1032
60	93	81	0.1048

3.4 FTIR Analysis

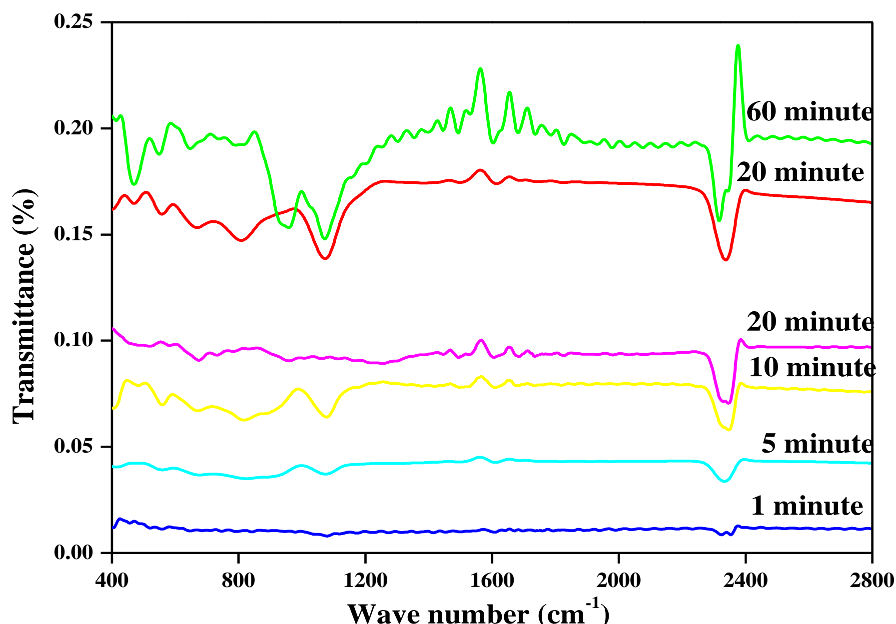

Figure. 7. FTIR spectra of HCl treated porous silicon for different etching time

Fig. 7 shows the FTIR spectra of HCl treated porous silicon samples prepared with different etching times. The observed surface bonding and their corresponding vibration modes are given in Table 3. The vibrational modes presented in Table 3 represent a clear silica fingerprint. Strong peaks were observed at 1085 cm^{-1} and some weak peaks of lower intensities were observed at around 422 cm^{-1}, 665 cm^{-1}, 808 cm^{-1} and 927 cm^{-1}. The strong peaks observed at 1085 cm^{-1} and 1405 cm^{-1} are assigned to the Si–O–Si stretching mode and CH_3 asymmetric deformation respectively. Other interesting characteristics are related to the oxidation and hydrogenation of the silicon matrix induced by the wet etching process.

The weak band at 808cm^{-1} can be attributed to the Si-H bending vibrational mode of SiH_2. These results indicate that the surface of PS contains the chemical species Si-H_n, which passivate the dangling bonds and play a key role in the efficiency of the luminescence process in porous silicon [20, 21]. The bending vibration of O in the Si-O-Si group is located at 422 cm^{-1} as a small double band.

The FTIR transmission peak intensity of Si-H_n complexes increases with increase in HCl treatment. The large hydrogen concentration in freshly prepared material has led to the suggestion that a silicon–hydrogen alloy effect is responsible for the luminescence.

© 2017 NSP
Natural Sciences Publishing Cor.

Table. 3: Observed surface bonding in the HCl treated Porous Silicon layer

Wave number (cm^{-1})	Bonds	Vibration mode
2358	Si-H	Stretching
2106	Si-H	Stretching
1405	CH_3	Asymmetric deformation
1085	Si-O-Si	Asymmetric stretching
927	$Si-H_2$	Scissors
808	$Si-H_2$	Vibration mode
664	Si-H	Wag
422	Si–O–Si	Bending

3.5 PL Analysis

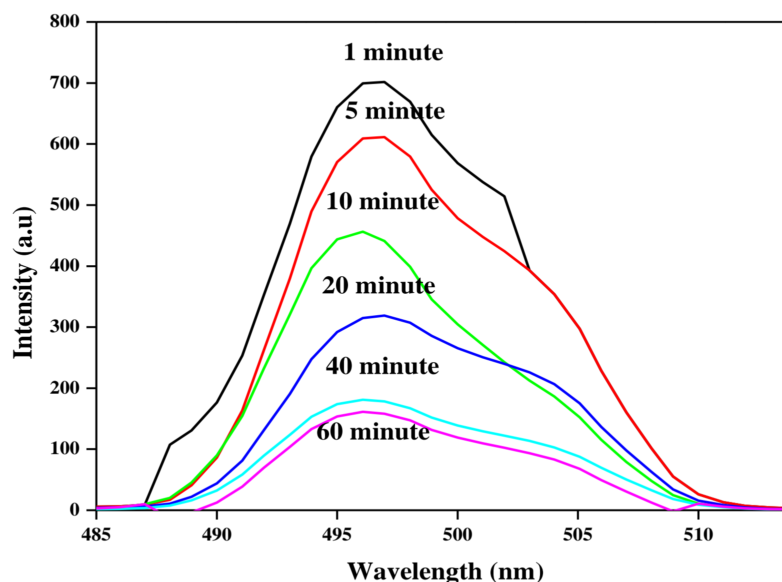

Figure. 8. PL spectra of HCl treated porous silicon for different etching time

Photoluminescence (PL) studies were carried out on chlorinated porous silicon to understand the effect of surface passivation on porous silicon. Treatment with HCl is found to produce the most efficient enhancement of the PL signal. Fig. 8 shows the PL spectra of HCl treated porous silicon samples for different etching time. The emission peak was found at about 498 nm for all the samples [22]. However, it can be seen that the PL emission intensity is drastically reduced on chlorination using HCl etching treatment. The occurrence of strong PL spectra at room temperature in the visible range may be attributed to the transitions among the quantum-confined states in nanoscale Si, which are influenced by the surface bond [23].

Hory *et al* [24] observed that when porous silicon is treated in boiling CCl_4, there is a net decrease in the concentration of the Si-H groups on the material surface, even without noticeable oxidation, and, in that case, a very large decrease in the photoluminescence intensity was also found.

4 Conclusion

Porous Silicon samples were prepared by electrochemical anodic etching of p – type (1 0 0) silicon wafers in a HF: Ethanol solution. The synthesized PS samples have been exposed to HCl solution for various etching time. SEM studies confirm the presence of silicon nanocrystallites and networks in the PS structure. EDAX spectra reveal chloride incorporation into the PS surface at strongly photoluminescent regions. Effective medium approximation method shows that the refractive indices of porous samples decrease with the growth of porosity. XRD study reveals that the crystallite size decreases as the etching time of HCl increases. FTIR results indicate that the surface of PS contains the chemical species $Si-H_n$, which passivate the dangling bonds and play a key role in the efficiency of the luminescence process in porous silicon. PL studies

© 2017 NSP
Natural Sciences Publishing Cor.

show that a strong visible emission peak is observed for all samples. The obtained variation of intensity in PL emission may be used for intensity varied light emitting diode applications. These results confirm that the PS is a versatile material with potential for optoelectronic application.

References

[1] L. T. Canham, Appl. Phys. Lett., Vol. 57, 1046 (1990).
[2] L. Pavesi, R. Guardini, Brazil. J. Phys., Vol. 26, No. 01, 152 (1996).
[3] M. A. Vasquez-A., G. AguilaRodriguez, G. Gracia-Salgado, G. Romero-Raredess, R. Pena-Sierra, Revista Mexicana De Fisca., Vol. 53, No. 06, 431 (2007).
[4] M. Voos, P.Huzan, C. Delalande, G. Bastard, Appl. Phys. Lett., Vol. 61, No. 10, 1213 (1992).
[5] Y M Weng, Zh N Fan, X F Zong. Appl. Phys. Lett., Vol. 63, No. 2, 168 (1993).
[6] I. Mihalcescu, M. Ligeon, F. Muller, R. Romestain, J. C. Vial, J. Lumin., 57 (1993)111.
[7] V. Agrawal, J. A. del Rio, Appl. Phys. Lett., Vol. 82, No. 10, 1512 (2003).
[8] R. S. Dubey, L. S. Patil, J. P. Bange, D.K. Gautam, Optoelectron and Adv. Mater.–Rapid Commun., Vol. 1, No. 12, 655 (2007).
[9] R. S. Dubey, D. K. Gautam, Optoelectron. Adv. Mater.–Rap.Comm., Vol. 1, No. 9, 436 (2007).
[10] J. E. Lugo, H. A. Lopez, S. Chan, P. M. Fauchet, J. Appl. Phys., Vol. 91, No. 8, 4966 (2002).
[11] S. Setzu, P. Ferrand, R. Romestain, Mater. Sci. & Engg., Vol. 70, No. 34 (2000).
[12] P. Ferrand, D. Loi, R. Romestain, Appl. Phys. Lett., Vol. 79, No. 19, 3017 (2001).
[13] C. J. Oton, L. Dal Negro, Z. Gaburro, L. Pavesi, A. Lagendijk, D. S. Wiersma, Phys. Stat. Sol., Vol. 197, No. 1, 298 (2003).
[14] B.Natarajan, N.Jayakumaran, S.Ramamurthy and V.Vasu, Surf.Rev.Lett. 15, 301 (2008).
[15] W.Thei, Surf.Sci.Rep., 29, No.3 (1999).
[16] J.J.Si, H.Ono, K.Uchida, S.Nozaki and H.Morisaki, Appl.Phys.Lett., 79, 3140 (2001).
[17] D.A.Bruggeman, Ann. Phys. (Leipz), 24, 636 (1935).
[18] H.Looyenga, Physica, 31, 401 (1965).
[19] D.Buttard, D.Bellet, T.Baumbach, Thin Solid Films, 276, 69 (1996).
[20] F. Namavar, H. P. Marushka, N. M. Kalkhoran, Appl. Phys. Lett.60, 2514 (1992).
[21] B. Natarajan, V. Vasu and S. Ramamuruthy, Proc.Int. Conf. Fiber Optics, Optoelectronis and photonics, Cochin University of Sci. Technol.101 (2004).
[22] I. Coulthard,W. J. Antel, Jr, J. W. Freeland, Appl. Phys. Lett., Vol. 77, No. 4 (2000).
[23] X. G. Zhang, J. Electrochem. Soc. 138, 3750 (1991).
[24] M. A. Hory, R. Herino, M. Ligeon, F. Muller, F. Gaspard, I. Mihalcescu, J. C. Vial, Thin Solid Films., 255, 200 (1995).

© 2017 NSP
Natural Sciences Publishing Cor.